Energy Reports 9 (2023) 4763–4780

Contents lists available at ScienceDirect

Energy Reports

journal homepage: www.elsevier.com/locate/egyr

Research paper

Techno-economic and GHG mitigation assessment of concentrated solar thermal and PV systems for different climate zones

Asad Ullah [a], Mariam Mahmood [a], Sheeraz Iqbal [b], Muhammad Bilal Sajid [a], Zohaib Hassan [a], Kareem M. AboRas [c], Hossam Kotb [c], Mokhtar Shouran [d], Bdereddin Abdul Samad [d,*]

[a] U.S-Pakistan Center for Advanced Studies in Energy (USPCAS-E), National University of Sciences and Technology (NUST), Islamabad, Pakistan
[b] Department of Electrical Engineering, University of Azad Jammu and Kashmir, Muzaffarabad 13100, AJK, Pakistan
[c] Department of Electrical power and machine Engineering, Faculty of Engineering, Alexandria University, Alexandria, Egypt
[d] Magnetics and Materials Research Group, School of Engineering, Cardiff University, Cardiff, UK

ARTICLE INFO

Article history:
Received 18 November 2022
Received in revised form 28 February 2023
Accepted 21 March 2023
Available online xxxx

Keywords:
Solar PV
Concentrated solar power
Techno-economic assessment
Sensitivity
Environmental sustainability

ABSTRACT

In this study, energy production by two solar energy technologies, namely concentrated solar power (CSP) and photovoltaic (PV) power, is compared from a technical, economic and environmental perspective. Initially, a 50 MW CSP plant is modeled and simulated at four selected sites in Pakistan. Then, the most feasible location of the CSP plant is compared with the solar PV plant of the same capacity. The effect of the solar thermal storage size and cooling system of the CSP system is investigated, while the photovoltaic tracking system is investigated to evaluate the technical and economic performance of the power plants. Technical performance is evaluated based on energy generation and capacity factors metrics, while economic performance is evaluated with respect to levelized cost, payback period and net present value. In addition, environmental criteria such as reducing greenhouse gas emissions (GHG), saving fossil fuels, and life-cycle water consumption are evaluated. From the results, it was concluded that the CSP plant located in Quetta is technically and economically viable. The capacity factor of the CSP plant is 36.6% compared to 19.8% for the PV plant, while the solar-to-electrical efficiency of the CSP plant is 14.2% compared to 20.8% for the PV plant. The required land area is 2.77 acres/GWh for the CSP plant and 2.33 acres/GWh for the PV plant, while the net capital cost of the CSP plant is five times higher than that of the PV plant. Various design parameters are optimized to obtain the minimum levelized cost of energy (LCOE) for both CSP and PV plants. The results of CSP and PV plants indicate that the LCOE can be reduced to 11.57 cents/kWh and 4.69 cents/kWh, respectively. Thus, the CSP plant performs better from the technical point of view while the PV plant performs better from the economic perspective.

1. Introduction

Energy is the main driving force of the global economy, and its demand is increasing day by day with the increasing population and industrialization (Department of Economic and Social Affairs, 2019). Fossil fuels are being depleted at a rapid rate. As of 2020, oil still holds the largest share at 31.2% of the global energy mix, followed by coal (27.2%), and natural gas (24.7%), while renewables hold a 5.7% share of primary energy consumption. The rapid rate of depletion and rising prices of fossil fuels, as well as the impact of greenhouse gases (GHGs), have led to an increasing global trend in the adoption of renewable energy resources. It should also be noted that while the world plans to move towards a carbon-neutral transportation system to meet its target of reducing greenhouse gas emissions, electric vehicles (EVs) will add 5% to global electricity demand by 2050 (Aksoy, 2009). To fulfill the 1.5 °C pathway, the electricity sector must be completely decarbonized by 2050, hence the need for an hour to ramp up renewables (IRENA, 2021).

According to the World Energy Outlook 2021, fossil fuel-fired thermal power plants emit about 40% of the 34.8 Gt of global carbon dioxide emissions, which must be reduced at a rapid rate (Cozzi and Gould, 2021). Therefore, low carbon energy production is a strategic priority to address climate change. Among

* Corresponding author.
E-mail addresses: asad.asadkhan908@gmail.com (A. Ullah), mariam@uspcase.nust.edu.pk (M. Mahmood), sheeraz.iqbal@ajku.edu.pk (S. Iqbal), mbilalsajid@uspcase.nust.edu.pk (M.B. Sajid), hzohaib94@gmail.com (Z. Hassan), kareem.aboras@alexu.edu.eg (K.M. AboRas), hossam.kotb@alexu.edu.eg (H. Kotb), shouranma@cardiff.ac.uk (M. Shouran), abdulsamadbf@cardiff.ac.uk (B. Abdul Samad).

https://doi.org/10.1016/j.egyr.2023.03.109

Abbreviations

AEP	Annual energy production
CF	Capacity factor
CSP	Concentrated solar power
CSTPP	Concentrated solar thermal power plant
DNI	Direct normal irradiance
GHG	Greenhouse gas
HTF	Heat transfer fluid
LCOE	Levelized cost of energy
NOCT	Nominal operating cell temperature
NPV	Net present value
PBP	Payback period
PV	Photovoltaic
SAM	System Advisor Model
SM	Solar multiple
STC	Standard test conditions
tCO_2	Tons of carbon dioxide
TES	Thermal energy storage
TMY	Typical meteorological year

the renewable resources, solar energy is an ideal choice for the world of the future because of its huge abundance, ease of hybridization, and cost-effectiveness in addition to the lack of harmful impact on the ecosystem (Kannan and Vakeesan, 2016).

Solar energy can be converted into electrical energy in two different ways: direct conversion through photovoltaics (PV) and indirect conversion through thermodynamic cycles. Despite the lower capital cost and other perks of a photovoltaic system, concentrated solar power (CSP) technology has many advantages such as better capacity factor, integration of TES to generate electricity during cloudy or after sunset hours, and ability to integrate with hybrid power systems. CSP costs have decreased by 50% over the past decade, and TES-equipped CSPs have been installed along PV systems to increase capacity factors and further reduce costs (Henner and REN21, 2017). There are four types of CSP technologies in use commercially: parabolic trough collector (PTC), solar tower (SPT), parabolic dish (PD), and linear Fresnel reflector (LFR).

CSP technology consists of concentrators to focus solar radiation onto a receiver containing a heat transfer fluid (HTF). HTF transfers heat to the working fluid of the power cycle to convert it into steam that drives the turbine to produce electrical power. Of all the four CSP technologies, the parabolic trough collector is the most mature and commercially available CSP technology (Ravi Kumar et al., 2021). The global installed capacities of PV and CSP systems in 2020 were 760 GW and 6.2 GW, respectively. In the CSP market, Spain and the United States account for nearly two-thirds of the global CSP capacity as shown in Fig. 1. Spain retained the world leader in operational capacity with 2.3 GW at the end of 2020, followed by the USA with nearly 1.7 GW From concentrated solar energy to commercial operation of power plants.

Boukelia et al. (2015) performed the optimization of a parabolic trough solar thermal power plant (PTSTPP) combined with thermal energy storage (TES) and fuel backup system (FBS) on two parameters: Solar Multiple (SM) and full load thermal energy storage (TES) to reduce LCOE and increase the annual energy yield. A study on the influence of meteorological parameters on the performance of a 50 MW CSP power station with cooling (dry and wet) and TES, has been performed under the climatic conditions of Tunisia, and a comparison of the performance with a reference station "Andasol-1" in Spain Trabelsi et al. (2016). The power plant with dry cooling system shows exceptionally good technical–economic performance and consumes 93.3% less water than the reference plant, and the levelized cost of electricity will be 1.45% lower. In the neighboring country of India, a study was conducted to assess the technical and economic potential of CSP systems based on the assessment of solar and ground energy resources across the country to identify suitable sites for CSP projects (Purohit and Purohit, 2017). Bishoyi and Sudhakar (2017) modeled a 100 MW solar thermal power plant with thermal energy storage at SAM and analyzed its performance to determine the economic feasibility of the project.

Kassem et al. (2017) conducted a comprehensive SWOT analysis of each CSP technology in the context of Saudi Arabia and combined the results of the analysis to assess the technical and financial performance of potential CSP scenarios. Belgasim et al. (2018) discuss the potential of CSP technology from the socio-economic perspective of Libya and assess the impact of different site criteria on its performance and implementation. The study shows that solar field installation contributes to 33% of the total cost of the project, thus, the economic competitiveness of CSP can be enhanced by encouraging locally manufactured components. Zubair et al. (2021) analyzed the trough-equivalent power plant to export power from Saudi Arabia to some Asian and European countries to meet peak load demand. Analysis based on the NPV, and standard cost confirms that exporting solar power from Saudi Arabia to much needed Pakistan is a viable proposition.

Soomro et al. (2019) investigated the potential, performance, and economic evaluation of four CSP technologies for different locations in Pakistan. Solar resource data, land topography, and water resources are key factors for evaluating the potential of CSP in this study. Through investigation, it was found that parabolic trough and solar power tower are feasible among all CSP technologies and had extraordinary performance during summer season. Crespi et al. (2020) analyzed the effect of pressure ratio and turbine inlet temperature on the thermal efficiency and work output of a supercritical carbon dioxide (sCO2) power cycle to evaluate its potential for CSP applications. Tahir et al. (2021) presented a technical–economic analysis of CSP for various potential sites with the objective function of reducing LCOE and discussed the potential barriers to its practical implementation.

Khalid and Junaidi (2013) conducted a sensitivity analysis of the economic feasibility of a 10 MW PV-based power plant with different array orientation patterns for Quetta. Mukisa et al. (2019) proposed a technique to determine the preferred roof area for solar PV installation and routing, moreover, they investigated the influence of loan period and loan share on project viability. Akhter et al. (2020) evaluated the performance characteristics of the installed PV system based on three different PV technologies (m-Si, p-Si and a-Si) for tropical climate regions. Alshare et al. (2020) compared the actual performance with the simulated results of a 5 megawatt photovoltaic system to relate its performance criteria to the climatic conditions in Jordan. Agyekum (2021) presented a detailed comparative technical–economic analysis of solar PV systems with tracking systems under different climatic conditions in Ghana. Pakistan is a developing country, where most of its energy demand is met by fossil fuels, which makes its energy market highly vulnerable to the international oil market. Thermal plants contribute a large percentage of the energy produced, while the contribution of renewable energy is only 3%, as shown in Fig. 2 (NTDC, 2021).

Hence, the expensive energy based on imported fuel affects the progress of various sectors and thus hinders economic growth. Therefore, there is a need for the hour to inject a large percentage of renewable energy into the country's energy mix. Pakistan has excellent potential for solar energy as it is located near the equator (Shabbir et al., 2020). The Alternative Energy Development

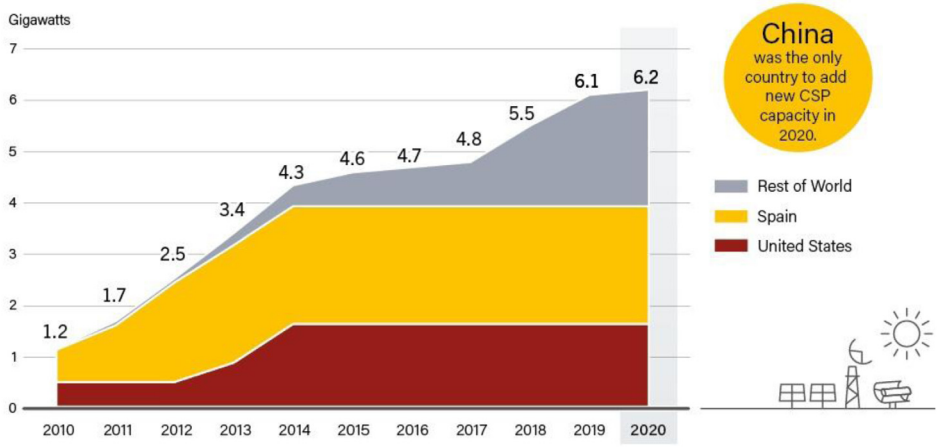

Fig. 1. Global installed capacity of concentrated solar power (CSP) (Henner and REN21, 2017).

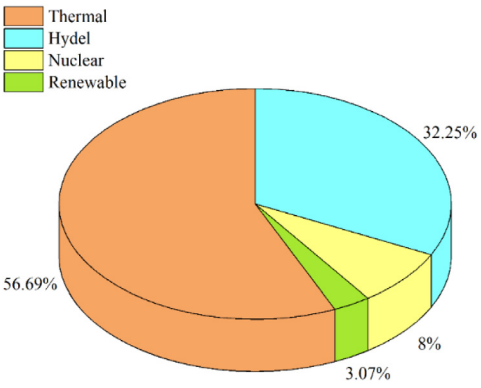

Fig. 2. Energy mix scenario of Pakistan (NTDC, 2021).

Board (AEDB) proposed the Alternative and Renewable Energy Policy (2019) to boost the share of renewable energy up to 30% by 2030 (Hall and Greeno, 2019). The installation of CSP technology on a utility scale will be a milestone for the promotion of the renewable energy sector. Therefore, it is very important for Pakistan to exploit the potential of solar energy resources for power generation purposes.

The aforementioned literature survey has certain limitations: The authors did not discuss any solar field size criteria: an optimal solar field maximizes energy production and reduces production cost. Previous studies did not carry a standard optimization to determine the lowest level energy cost (LCOE) and optimal TES size against each SM with exact input variables according to the reference site. This study seeks to definitively address all of these issues. In this paper, a comprehensive economic analysis is presented based on realistic cost values taking into account all types of taxes and incentives. Furthermore, environmental analysis is performed on RETScreen to determine the reduction of greenhouse gases and their impact on the environment. In the end, an accurate comparison of CSP and PV systems is drawn based on performance, financial and environmental perspectives, to find the positives and comprehensiveness. The main objectives of this research work are:

- Performance analysis of a 50 MW CSP plant under different climatic zones.
- Techno-economic and environmental assessment of CSP and PV systems for a suitable location.
- Optimization of different design parameters to minimize the LCOE for both CSP and PV plants.

2. Methodology

In this study, the CSP-based power plant is modeled on the System Advisor Model (SAM). Initially, four different sites were selected on the basis of climatic zones. The CSP-based power plant was designed, and the results simulated for one year. Then, parametric analysis is performed on the basis of various input parameters such as solar multiple (SM), thermal energy storage (TES), loop inlet/outlet temperature, turbine output fraction, and initial temperature difference (ITD) at the design point to obtain Minimize AEP and LCOE. The most feasible site for a CSP-based power plant is compared with a PV system of equivalent capacity. Fig. 3 shows the approach adopted in this methodology.

2.1. CSP modeling

A CSP system of 50 MW capacity is modeled in SAM at four selected sites for CSP deployment. The gross to net conversion factor is kept around 0.9 because it is assumed that output is reduced by 10% due to parasitic losses. Three main components of CSP plants as shown in Fig. 4 are the solar field, thermal storage and power block. CSP technology uses mirrors to focus the solar beam radiation onto a receiver. The receiver, which contains a fluid, converts the radiation into thermal energy. This heat energy is then transferred by the heat transfer fluid to the working fluid in the Rankine cycle, which converts it into steam to drive the turbine to generate electricity. This thermal energy can also be stored in the TES storage medium for later use during hours without sunlight. The design point parameters of these components are discussed in the following sections, while all the remaining technical parameters are described in Table 3.

2.1.1. Meteorological data

Climatic conditions play a pivotal role in the performance of solar thermal power plants. The required meteorological data to analyze and simulate the performance of solar thermal power plants are solar irradiation, ambient temperature, wind speed, air pressure, and relative humidity. Moreover, dry-bulb and wet-bulb temperature data required to model and compare the performance of dry and wet cooling systems for CSP power plants is obtained from the Pakistan Meteorological Department (PMD). DNI is essentially focused by CSP technology to produce thermal energy while GHI is focused by PV technology to generate electricity. Pakistan has a high potential for deploying CSP technology across the country, especially in northwestern Baluchistan as shown in Fig. 5. Moreover, Fig. 6 shows the monthly variation in DNI of selected sites for CSP deployment, while Fig. 7 shows the monthly variation in ambient temperature and wind speed for four selected sites.

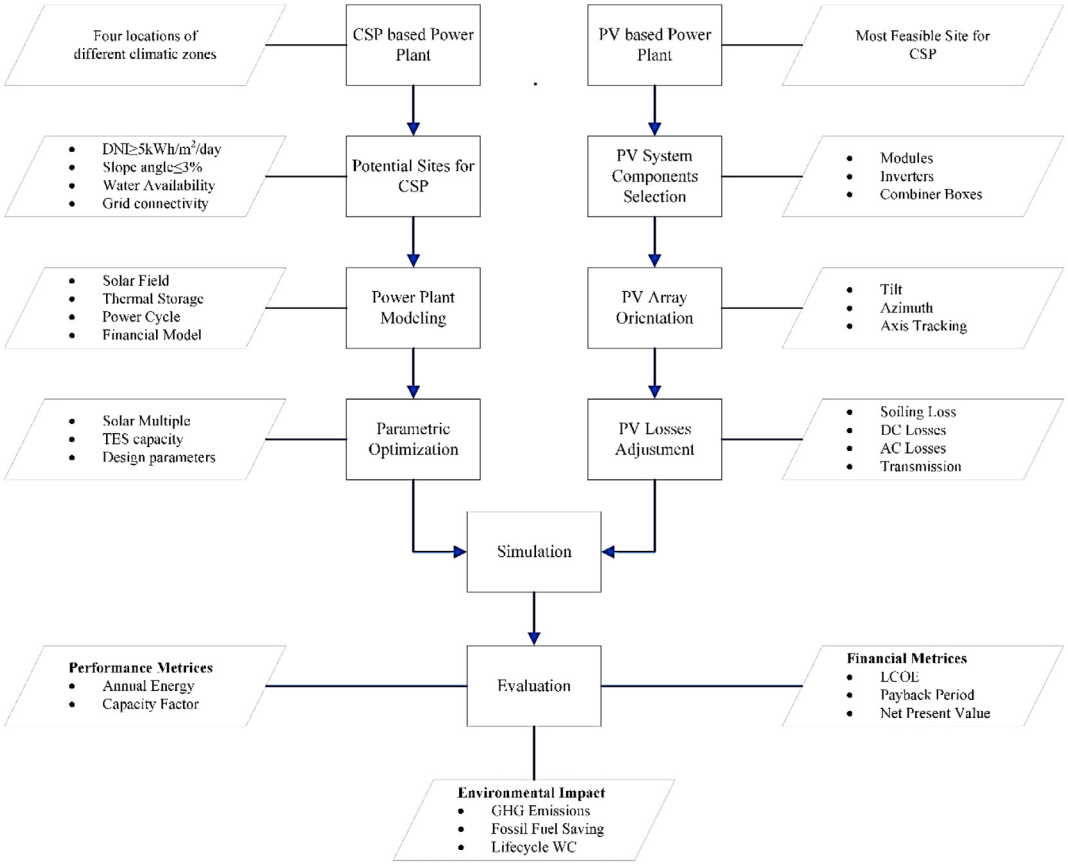

Fig. 3. Methodology for identifying the feasible site for CSP deployment.

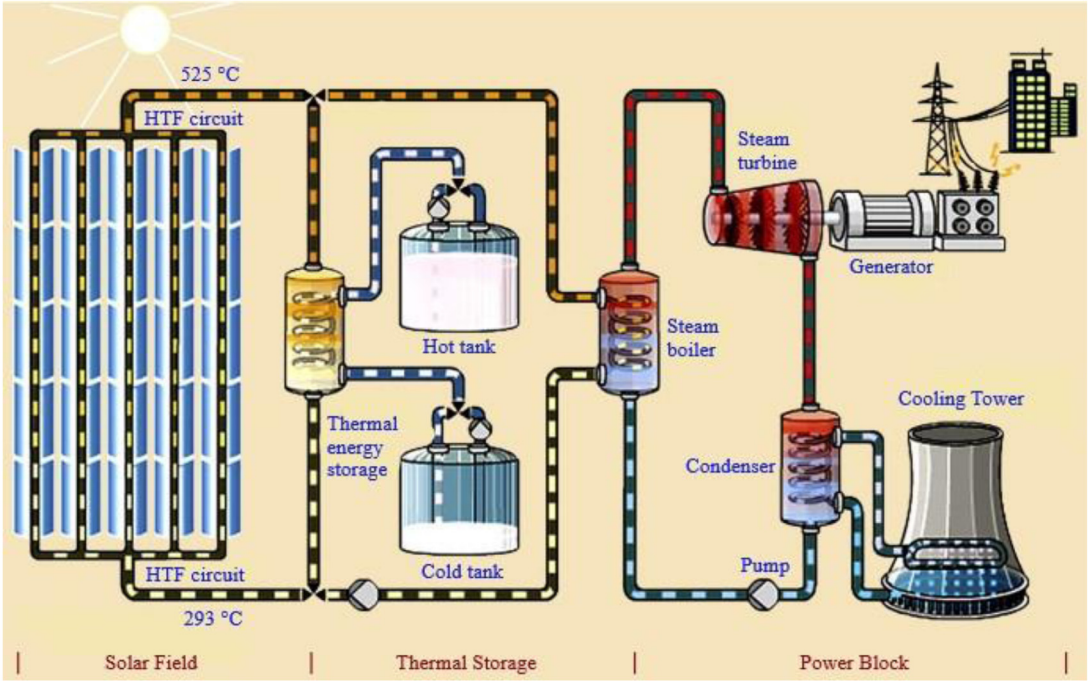

Fig. 4. Structure of a concentrated solar power plant.

2.1.2. Site selection

The first step towards building a CSP based power plant is site selection. Literature suggests that CSP based power generation is technically and economically feasible for locations receiving DNI greater than 1800 kWh/m^2/year (DNI $\geq$ 5 kWh/m^2/day). Under the ESMAP program of the World Bank, Renewable Energy Resource Mapping Initiative of Pakistan is launched to boost the growth rate via sustainable energy solutions. This mapping

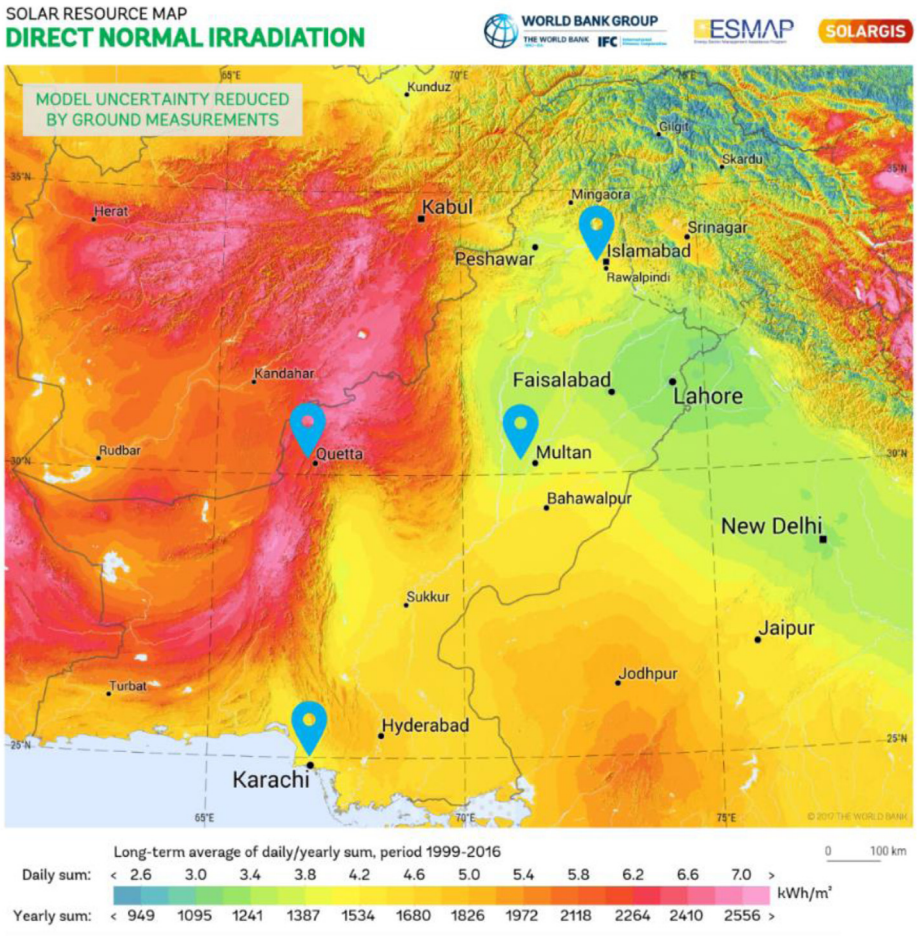

Fig. 5. Direct Normal Irradiance (DNI) solar map of Pakistan (Rule, 2013).

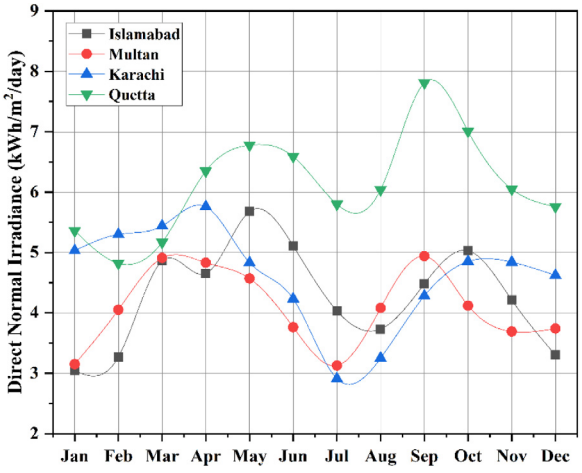

Fig. 6. Monthly average direct normal irradiance (DNI) of selected sites.

indicates that 83% area of the country exceeds the DNI threshold of 2000 kWh/m^2/year, while peak DNI values, surpassing 2700 kWh/m^2/year, can be observed in the northwestern part of Schillings and Stokler (2015) as shown in Fig. 5. Secondly, there should be vast barren land with no or less than 3% slope angle as it has a significant impact on the output of CSP based power generation system. Typical Meteorological Year (TMY) data that represents median weather conditions is used to evaluate the performance of CSP plants of selected sites. The selected sites of Pakistan receive 7–11 sunshine hours (daily) throughout the year. The solar irradiance data of selected sites is shown in Table 1. There are lots of other considerable factors such as appropriate infrastructure, water availability, and grid connectivity.

2.1.3. Solar field sizing

The solar field is the heat-collecting section of the plant that comprises parallel loops of solar collector assemblies (SCAs) of the parabolic trough. A common header pipe supplies each loop with an equal amount of flow rate of heat transfer fluid (HTF), and another header pipe collects the hot HTF to deliver it either directly to the power cycle for power generation or to the TES system for later use. The solar field is usually divided into multiple sections to minimize pumping pressure losses.

An optimal solar field size maximizes the time over a year during which it generates enough thermal energy to run the power block at its rated capacity, minimizes the capital and operating cost, and utilizes the thermal energy storage effectively. Irradiation at design point determines the solar field size. Using too low reference direct normal irradiance (DNI) results in excessive dumped energy while using too high results in an undersized solar field that is unable to meet the rated capacity of the power block most of the time.

2.1.4. HTF selection

Two commonly used HTFs in CSP generation are HITEC Solar Salt and Therminol VP-1. Their properties are characteristics are described in Table 2.

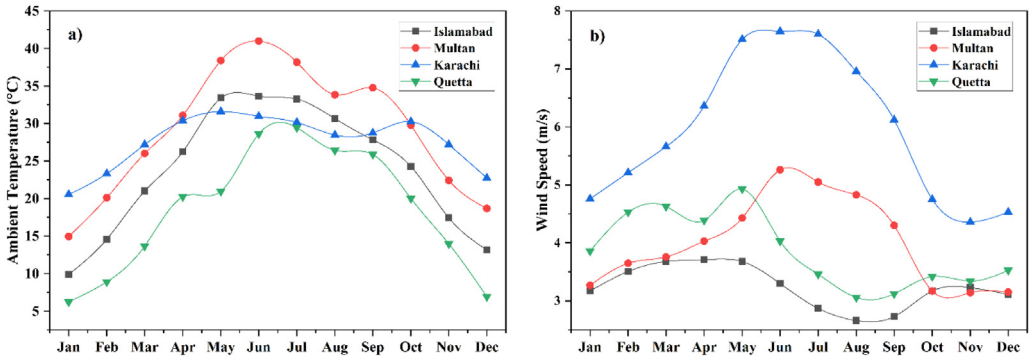

Fig. 7. Monthly average (a) ambient temperature and (b) wind speed of selected sites.

Table 1
Coordinates and climate description of selected sites.

Location	Latitude	Longitude	DNI (kWh/m^2/year)	Sunshine hours (annual)	Ambient temp (°C)	Climate zone
Islamabad	33.65°N	73.05°E	1565.41	2945	23.8	Sub-mountains with mild cold climate
Multan	30.15°N	71.45°E	1488.98	3100	29.1	Dry and hot region with arid climate
Karachi	24.85°N	67.05°E	1681.19	2950	27.6	Coastal area with warm humid sub-tropical climate
Quetta	30.15°N	67.01°E	2238.94	3340	18.9	High elevation with cold semi-arid climate

Table 2
Properties of potential HTFs for concentrated solar thermal power generation (Bishoyi and Sudhakar, 2017).

HTF	Min. Temp (°C)	Max. Temp (°C)	Specific heat (kJ/kg °C)	Density (kg/m^3)
Hitec solar salt	238	593	1.561	1790.2
Therminol VP-1	12	400	1.532	1067.6

Hitec Solar Salt is a ternary mixture of 53% KNO_3, 40% $NaNO_2$, and 7% $NaNO_3$. Hitec Solar Salt has higher operating temperature and thermal conductivity, being more energy-dense, less viscous, non-toxic, and lower cost than thermal oil making it suitable for HTF. The HTF with lower freezing temperature causes lower thermal energy losses (Sau et al., 2016). The loop outlet temperature is achieved by varying either HTF mass flow rate, velocity, or by number of SCAs. The loop mass flow rate and velocity of HTF are calculated from Eqs. (1) and (2), respectively.

$$\dot{m} = \frac{A_{SCA}\eta_{abs}N_{SCA}I_b}{C_P \Delta T} \tag{1}$$

$$v = \frac{4\dot{m}}{\rho.\pi.{D_{abs}}^2} \tag{2}$$

where A_{SCA} is the area of collector, η_{abs} is the absorber efficiency, N_{SCA} is the number of collector assemblies, I_b is the DNI at design point, C_p is the specific heat, ρ is the density, D is the diameter, and ΔT is the temperature rise across the loop.

2.1.5. TES design

Renewable energy power plants are subject to weather transitions and CSP technology can store energy cost-effectively in TES to overcome this problem. TES is an essential key component of CSP technology to improve its reliability, capacity factor, dispatch strategy, and efficiency. It consists of three main parts: a storage tank, a storage medium, and a heat transfer mechanism. Hitec solar salt is selected as storage medium since it has relatively higher density. Sensible heat storage (SHS) is most widely used in utility-scale CSP plants due to its low cost, straightforward method, reliability, and experimental feedback. Thus, a two-tank TES system is modeled; one to store hot fluid while the other to collect cold fluid.

2.1.6. Power block

The power block subsystem converts thermal energy from the solar field into electrical or mechanical energy. It works on superheated steam Rankine cycle with feed water heating and implements a statistical design of experiments (DOE) approach to determine the cycle behavior (Wu and Hamada, 2011). This power cycle unit can either be stand-alone or integrated with a combined cycle to either offset fossil fuel usage (Dersch et al., 2004) or boost power (Elmohlawy et al., 2019). The thermal efficiency of the power block is linked to the inlet temperature of the Rankine cycle.

2.2. PV modeling

A photovoltaic system of 50 MW nominal power is modeled in SAM at the most feasible location for CSP power plant. The design parameters of PV plant are described in Table 5. Since grid connected utility-scale systems directly feed the power into the electricity grid, they do not necessarily need the expensive battery storage.

The following steps are followed for modeling the PV plant.

- Specify the location and import its weather data resources.
- Select the PV system components such as modules and inverters.
- Define the PV array orientation such as tilt and azimuth angles.
- Adjust different types of system losses and degradation rate.
- Determine system cost values and financial parameters.
- Define the method of metering, billing and electricity prices.

2.2.1. PV system description

The PV system consists of 124,896 monocrystalline silicon modules of Jinko solar company, with rated power of 400 W_{dc} and 678 inverters of SMA America with each maximum AC power of 62 500 W_{ac}. The detailed specifications of the module and inverter are shown in Table 4. The nominal efficiency of each module is 20.85% at standard test conditions (STC) of 1000 W/m^2

Table 3
Design point and technical parameters of CSP plant.

Parameter	Value	Parameter	Value
Location and Resource		Number of modules per assembly	8
Location	Quetta	**Receivers (HCEs)**	
Latitude & Longitude	30.18°N,66.98°E	Receivers	Schott PTR70 2008
Average DNI	6.13 kWh/m^2/day	Absorber tube inner diameter	0.066 m
System Design		Absorber tube outer diameter	0.07 m
Solar Multiple	2	Glass envelope inner diameter	0.115 m
Cycle thermal power	156 MWt	Glass envelope outer diameter	0.12 m
Field thermal power	312 MWt	Absorber flow pattern	Tubular flow
Design point DNI	850 W/m^2	Absorber material type	304 L
Loop inlet HTF temperature	293 °C	Annulus gas type	Hydrogen
Loop outlet HTF temperature	525 °C	**Thermal Storage**	
Solar Field		Storage HTF fluid	Hitec Solar Salt
Row spacing	15 m	Full load hours of TES	6
Stow and deploy angle	170° and 10°	Storage volume	5241.4 m^3
Water usage for wash	0.7 L/m^2	Parallel tank pairs	1
Washes per year	63	Pumping power for HTF	0.15 kJ/kg
Actual number of loops	98	Cold tank heater set point	250 °C
Total aperture reflective area	514 304 m^2	Hot tank heater set point	365 °C
SCA/HCE assemblies per loop	8	**Power Cycle**	
Total land area	445 acres	Cycle gross output	55.5 MW
Heat Transfer Fluid (HTF)		Gross to net conversion factor	0.9
Heat transfer fluid	Hitec Solar Salt	Estimated net output	50 Mwe
Field HTF min operating temp.	238 °C	Cycle thermal efficiency	0.356
Field HTF max operating temp.	593 °C	HTF hot temperature	525 °C
Freeze protection temp.	150 °C	HTF cold temperature	293 °C
HTF pump efficiency	0.85	Boiler operating pressure	100 bar
Collectors (SCAs)		Condenser type	Air-cooled
Collectors	SkyFuel SkyTrough	**Parasitic Losses**	
Reflective aperture area	656 m^2	Piping thermal loss coefficient	0.45 W/m^2-K
Aperture width	6 m	Balance of plant parasitic	0.02467 Mwe
Length of collector assembly	115 m	Aux heater boiler parasitic	0.02273 Mwe

Table 4
PV system module and inverter specifications.

Parameter	Value	Parameter	Value
Module			
Jinko Solar Co. Ltd.	JKM400M-72L	V_{mp}	41.7 V
Technology	Mono-c-Si	I_{mp}	9.6 A
Maximum Power (Pmax)	400.32 W_{dc}	V_{oc}	49.8 V
Nominal efficiency	20.85%	I_{sc}	10.36 A
NOCT	45 ± 2 °C	Temp coefficient at Pmax	−0.406%/°C
Inverter			
SMA America	STP 60-US-10 [480 V]	Nominal AC voltage	480 Vac
Weighted Efficiency	98.434%	Nominal DC voltage	710 Vdc
Maximum AC Power	60 000 W_{ac}	Maximum DC voltage	800 Vdc
Maximum DC Power	60 974.6 W_{dc}	Maximum DC current	85.879 A_{dc}

solar irradiance and 25 °C cell temperature, while the weighted efficiency of each inverter is 98.434%. The performance of the PV module strongly depends on the intensity of irradiance as shown in Fig. 8.

2.2.2. PV field description

There are 7806 strings in parallel with each string consisting of 16 modules. Modules are connected in series to increase the voltage up to the minimum operating requirement while strings are connected in parallel using a combiner box to meet the current requirement. As Pakistan is located in the northern hemisphere, the parallel PV arrays are placed in an east–west orientation with due south facing (Azimuth 180°) at which PV systems have maximum annual energy yield. The parametric simulation is run to find the optimum tilt angle for the PV field. The azimuth angle of 180° for facing true south and tilt angle of 31° are selected to evaluate the performance of the PV system. In case of a tracking system, EW tracking performs better than NS tracking for solar irradiance in Pakistan (Sadati et al., 2015).

2.2.3. PV performance parameters

International Energy Agency (IEA) has established PV system performance parameters, described in IEC standard 61724, which

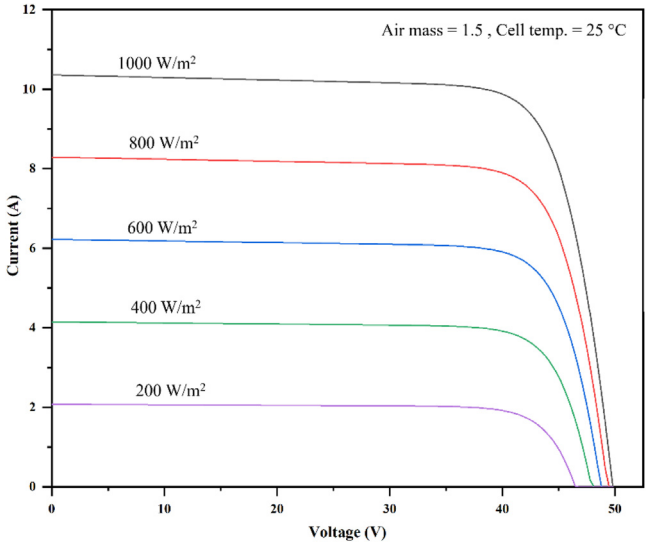

Fig. 8. The I-V characteristic curve at STC of PV module.

Table 5
Design parameter for PV plant.

Parameter	Value	Parameter	Value
Rated Capacity	50 MW	**Inverter**	
Tilt angle	31°	Number of inverters	667
Azimuth angle	180°	Total AC capacity	41,688 kW
Total land area	201 acres	Total DC capacity	42,909 kW
Modules		Max DC voltage	800 V
Number of PV modules	124,896	Min MPPT DC voltage	500 V
Modules per string	16	Max MPPT DC voltage	800 V
Strings in parallel	7806	**Overall System**	
String open circuit voltage	796.8 V	Derating factor	80%
String max power voltage	667.2 V	Ground reflectance	20%
Total module area	239,800 m^2	Degradation rate	0.5%/year

are utilized in this study to evaluate the operational and reliability performance of grid-connected PV systems. These parameters include energy output, energy yields, system efficiency, array capture loss, capacity factor (CF), and performance ratio (PR). The output of PV module depends on solar irradiance and temperature, is calculated from Eq. (3). Where P_{NP} is the nameplate capacity, f_{PV} is the derating factor, G_T is the incident solar radiation, α is the temperature coefficient, T_C is the cell temperature, and T_{STC} is the cell temperature at STC.

$$P_{PV,out} = P_{NP} f_{PV} \times \left(\frac{G_T}{1000}\right) \times [1 + \alpha\,(T_C - T_{STC})] \tag{3}$$

All the concerning PV system performance parameters are defined in Table 6.

2.2.4. PV system losses

The losses occur in different components of the PV system during the energy conversion process and affect the performance of the PV system output. These are array losses L_A and system losses L_S are defined below.

I. Array losses (L_a): The losses occurred in the PV array during the conversion of solar energy into DC energy, are defined as array losses.

$$L_A = Y_r - Y_a \tag{4}$$

These losses have further two types.

(a) Thermal capture losses (L_{CT}): These losses occur due to higher cell temperature than STC.
(b) Miscellaneous capture losses (L_{CM}): These losses occur due to mismatching, wiring, shading, soling, string diodes, and MPPT errors.

II. System losses (L_S): System losses are defined by the difference between array yield and final yield. These losses occur during the conversion of DC energy into AC energy by the inverter.

$$L_S = Y_a - Y_f \tag{5}$$

2.2.5. Financial model

The financial model calculates financial metrics for CSP and PV systems based on variations in cash flows of power project over an analysis period. For the distributed generation financial model, the renewable energy project reduces grid power purchases to meet the required electric load of a building or facility. If there is no load, then all the system generated power is considered excess power generation that is either credited for net metering or sold for buy all/sell all mode to the grid by the project. This section provides insight into different economic parameters to determine the financial viability of the project. System cost includes all the direct and indirect capital costs that defines the installation and operating cost of the project. Shown in Table 7 are system cost parameters for both solar technologies, while Table 8 demonstrates the financing cost and other financial parameters of the project according to monetary policy of State Bank of Pakistan (SBP) (State Bank of Pakistan, 2014). There is no CSP plant practically working or under construction in Pakistan. So, its system cost is considered in context of IRENA reports and already published work, While there are plenty of independent power producers (IPPs) for PV who are already working or have submitted their tariff petition applications to NEPRA (2020, 2021).

The government of Pakistan offers plenty of fiscal and financial incentives to encourage investment in the renewable energy sector, such as income and sales tax exemption, no customs duty and premium tariff rates (GoP, 2006; Policy, 2020). So, tax depreciation of any kind is not included in this economic model. Moreover, the tariff paid to independent power producers (IPPs) is on an upward trend. So, an electricity bill escalation rate of 10% per year is chosen for this project.

Financial evaluation is done on basis of the following three metrics:

i. Levelized Cost of Energy (LCOE)

LCOE determines the total project lifecycle cost per kilowatt-hour ($/kWh). It is the minimum cost at which electricity can be sold over the lifetime of the project to achieve break-even point.

$$LCOE = \frac{-C_0 - \frac{\sum_{n=1}^{N} C_n}{(1+d_{nominal})^n}}{\frac{\sum_{n=1}^{N} Q_n}{(1+d_{real})^n}} \tag{6}$$

where Q is the electricity generated, C is the annual cost, C_0 is the equity investment amount, d is the discount rate, n is the number of years, and N is the analysis period of the project.

ii. Net Present Value (NPV)

NPV determines the economic feasibility of the project based on assessments of both revenues and costs. A positive NPV indicates that the project is feasible.

$$NPV = \sum_{n=0}^{N} \frac{C_n}{(1 + d_{nominal})^n} \tag{7}$$

where C_n is the after-tax cash flow in year n, d the is discount rate, and N is the analysis period of the project.

iii. Payback Period (PBP)

The payback period is the time taken by the project to regain the initial investment; from the revenue it produces.

$$PBP = \frac{Initial\ Investment\ Cost}{Annual\ Savings} \tag{8}$$

3. Results and discussions

A study of 50 MW solar thermal power plant in four different climatic zones is performed in SAM. The performance of solar

Table 6
PV system performance parameters (Akhter et al., 2020; Alshare et al., 2020; Ahmed et al., 2021).

Parameter	Definition	Equation	Units
Array yield (Y_a)	The ratio of DC energy output to the rated power of the PV system for a specific period	$Y_a = E_{dc}/P_{rated}$	kWh/kW
Final yield (Y_f)	The ratio of AC output energy to the rated power of PV system at standard test conditions (STC) for a specific period	$Y_f = E_{ac}/P_{rated}$	kWh/kW
Reference yield (Y_r)	The ratio of total in-plane solar radiation (kWh/m^2) to the reference solar irradiance (1 kW/m^2) over a given period	$Y_r = H_t/G_r$	kWh/kW
Performance ratio (PR)	The ratio of final yield to reference yield	$PR = Y_f/Y_r$	%
Capacity Factor (CF)	The ratio of the energy output of the PV system to the energy output when the system is running at its maximum capacity over a period	$CF = \frac{E_{ac}}{P_{rated} * 8760}$	%
Module efficiency	The ratio of energy converted by a photovoltaic module to the solar radiation	$\eta_{pv} = \frac{E_{dc}}{H_t * A_m}$	%
Inverter efficiency	The ratio of AC power generated by an inverter to the DC power produced by the PV array	$\eta_{inv} = \frac{P_{ac}}{P_{dc}}$	%
System efficiency	The product of module efficiency and inverter efficiency	$\eta_{sys} = \eta_{pv} * \eta_{inv}$	%

Table 7
Various cost parameters (Awan et al., 2019; Hirbodi et al., 2020; Ali and Khan, 2020; Ahmed et al., 2021; Tahir et al., 2021).

Parameter	Value	Parameter	Value
CSP		**PV**	
Solar field	150 \$/m^2	Module	0.43 \$/W$_{dc}$
HTF	60 \$/m^2	Inverter	0.12 \$/W$_{dc}$
TES	65 \$/kWh$_t$	Balance of system	0.18 \$/W$_{dc}$
Power plant	1050 \$/kW$_e$	Installation labor	0.11 \$/W$_{dc}$

Table 8
Financial parameters.

Parameter	Value	Parameter	Value
Analysis period	25 years	Debt percent	100%
Inflation rate	2.5%	Loan term	10 years
Nominal discount rate	9.06%	Loan rate	5%
Insurance rate	1%		

thermal power plants installed at selected sites is predicted by SAM's physical trough model. This model assumes that flow is unidirectional and heat transfer is in a radial direction for the receiver. For the collector, it accounts for the losses like geometry defects, tracking error, incidence angle modifier, shadowing, mirror reflectance, and soiling. TES is designed to store excessive thermal energy and run power cycle at its rated capacity. The plant is simulated for a period of one year for each potential zone and then the performance of the most feasible site for CSP is compared with the same capacity of PV for that location. In the end, emission analysis is performed on RETScreen.

3.1. Performance evaluation of the CSP

The monthly energy production along the capacity factor of four potential sites is shown in Fig. 9. It indicates that monthly energy production is significantly higher during months of higher DNI and number of sunshine hours. All the sites have produced maximum energy from April to September due to relatively higher DNI in this span. Thus, the energy produced by the CSP plant and capacity factor is hugely dependent on the value of DNI. For example, in Multan, the highest energy 14.13 GWh is produced in April with a capacity factor of 39.25% while the lowest energy 3.81 GWh was produced in January with a 10.24% capacity factor. For Islamabad, the highest energy 17.35 GWh is produced in May with a capacity factor of 46.65% while the lowest energy 2.69 GWh was produced in December with a 7.24% capacity factor. For Karachi, the highest energy 16.76 GWh is produced in April with a capacity factor of 46.54% while the lowest energy 6.76 GWh was produced in July with an 18.17% capacity factor. For Quetta, the highest energy 18.84 GWh is produced in September with a capacity factor of 52.34% while the lowest energy 7.52 GWh was produced in December with a 20.22% capacity factor. It is observed that months of higher average DNI and longer sunshine hours produce significantly higher energy and give higher capacity factor. For instance, Karachi experiences lowest DNI of 2.91 kWh/m^2/day and total 155 sunshine hours in July results in lowest monthly energy production of 6.76 GWh. On the other hand, Quetta experiences highest annual DNI of 2239 kWh/m^2 and sunshine hours of 3340 among the selected sites. Thus, the overall CSP performance is better in Quetta because of higher solar irradiance, longer sunshine duration, lower ambient temperature, and lower humidity.

The annual energy production, capacity factor, and water usage of CSP based power plants at four potential sites are shown in Table 10. Simulation results indicate that CSP based power plant in Quetta can produce annual energy of 160.31 GWh with a capacity factor of 36.6%, followed by a power plant in Karachi which can produce annual energy of 129.26 GWh with a capacity factor of 29.5%. The power plant in Islamabad can produce annual energy of 113.42 GWh with a capacity factor of 25.9%, and 112.04 GWh with a capacity factor of 25.6% can be produced in Multan. The annual water consumption for these four sites ranges from 36,000 m^3 to 40,000 m^3.

System power generation trend varies every day for each location according to TMY weather data. The Fig. 10 shows the variation of system power generation in different seasons of Pakistan. Although DNI is available in the morning, yet system starts generating power a bit late because HTF needs to reach a specific temperature and power block needs to fulfill the minimum turbine output fraction condition before it starts producing power. Similarly, there is a notable dip in the late hours of the day because there is a temperature drop in HTF when TES starts functioning. The solar field thermal output increases due to higher intensity and longer duration of solar irradiance in June and September, consequently the duration of power plant operation hours is notably increased in these respective months. This highlights the significance of TES in seasons of higher average DNI, particularly in spring, summer and fall for Quetta.

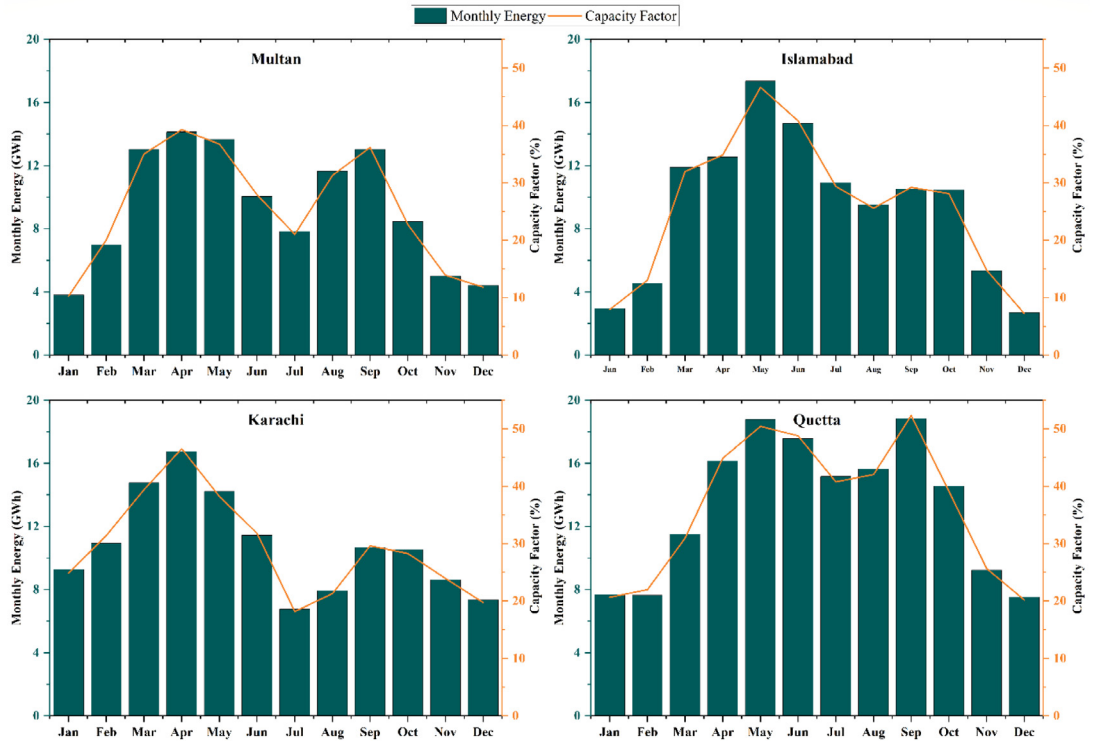

Fig. 9. Monthly power generated and capacity factor from 50 MW CSP plant in selected sites of Pakistan.

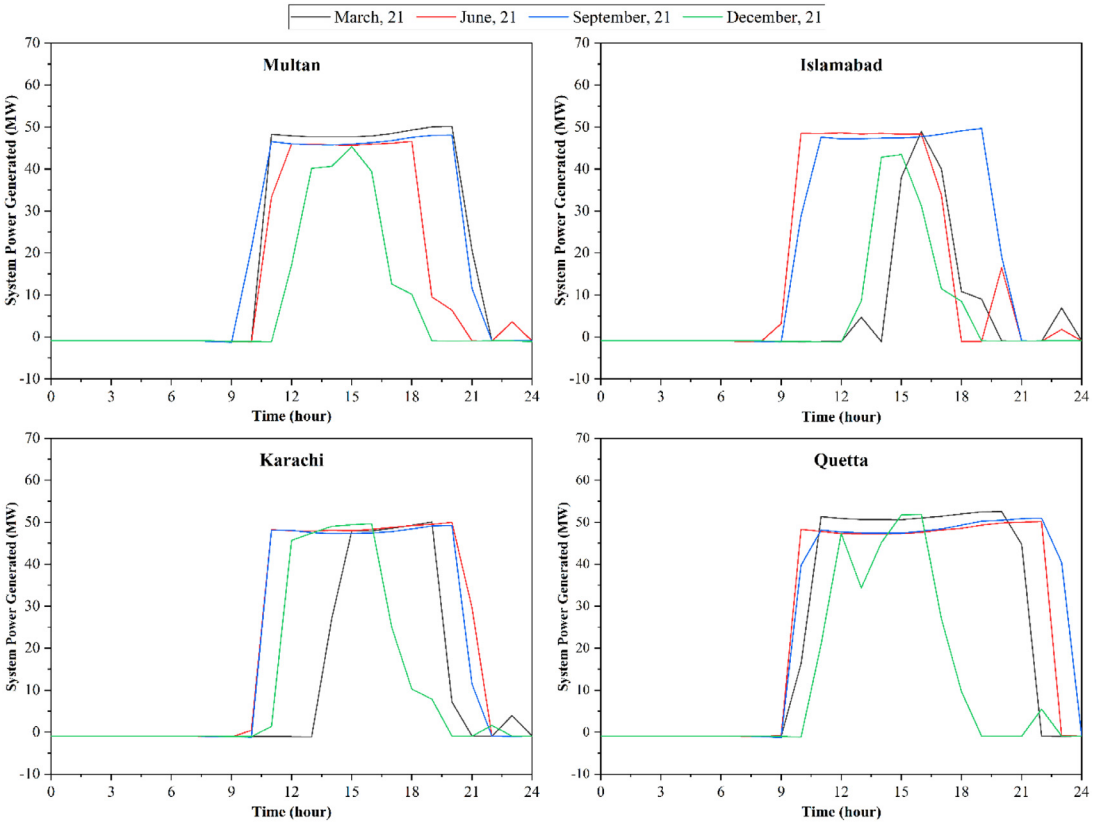

Fig. 10. Seasonal variation in system power generation trend of CSP plant for selected sites.

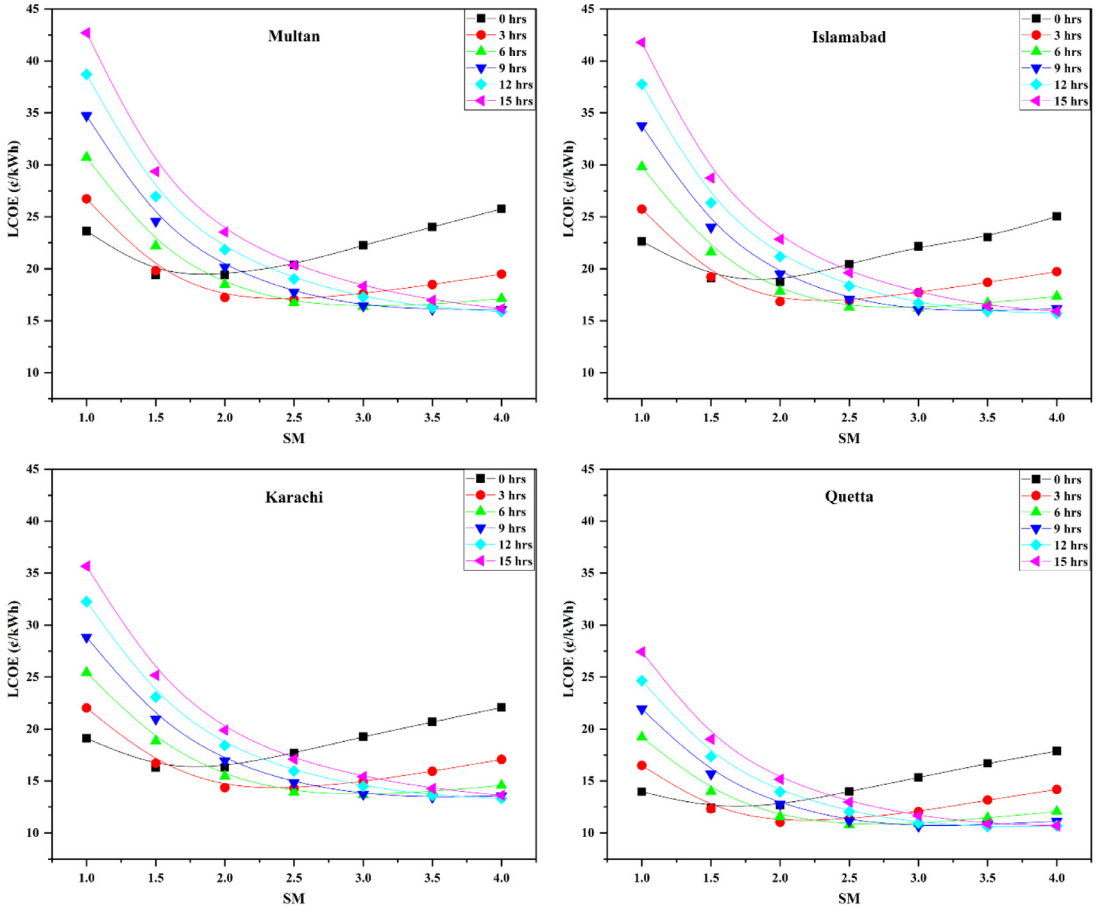

Fig. 11. The impact of SM and TES on LCOE of selected sites for CSP plant.

3.2. Economic evaluation of the CSP

The aim of the economic assessment is to evaluate the feasibility of solar power plants. The economic feasibility of solar power plants is evaluated in terms of LCOE, NPV, and PBP. The values of financial parameters are mentioned in Table 8. The optimization of LCOE is performed by varying SM from 1 to 4, and TES from 0 to 15 h. The Fig. 11 shows the LCOE at different SM and TES hours. For the most feasible site Quetta, the lowest LCOE of 10.51 cents/kWh can be achieved at SM of 3.5 and TES of 12 h.

These results show that LCOE with a fixed TES starts to decrease with increasing SM until it achieves a minimum value, and then it starts increasing gradually. As LCOE depends on plant installation costs and amount of power generation. This is due to the reason that installation, operation, and maintenance costs of the power plants increase linearly with increase in solar field size. On the other hand, field thermal and fluid losses increase more rapidly with increase in solar field size. That is why the LCOE increasing trend is observed at higher SM since a bigger solar field attributes to enormous fluid and thermal losses. Thus, there is an optimal SM for each TES capacity at which minimum LCOE can be achieved. This minimum LCOE occurs at a higher SM for a CSP plant with a larger TES capacity. Since large-scale CSP plants are economically viable, LCOE will start decreasing with increasing power plant capacity. Similarly, solar-to-electricity efficiency (SEE) starts increasing with SM until it reaches a maximum value, and then it starts decreasing. Similarly, the Payback period starts to decrease with the increase of Solar Multiple to an extent. After that, it starts increasing gradually.

The results indicate that Quetta is the most suitable location for CSP plant among these four sites, because of its highest AEP and lowest LCOE with 86.2% factor of gross to net conversion and 7.7 years of payback period.

3.3. Sensitivity analysis of the CSP

Sensitivity analysis is used to depict the sensitivity of focused metrics to various inputs. The figures below show the effect of the inflation rate and discount rate on the economic viability of the project. Sensitivity analysis is performed by varying the inflation rate from 1.0 to 4.0% and the discount rate from 7.0 to 12.0%. The Fig. 12 indicates that an increase in the inflation rate from 1.0 to 4.0% results in a decrease in LCOE from 13.06 ¢/kWh to 10.21 ¢/kWh and an increase in NPV from 477 to 833 million US$. This is because of government's subsidies to power producers due to upsurge in inflation rate. On the other hand, an increase in the discount rate results in an increase in LCOE and a decrease in NPV. The sensitivity analysis performed on loan rate indicates that LCOE increases with increase in loan rate, while it decreases with loan term as shown in Fig. 13. The behavior of increasing LCOE is due to the reason that loan rate increases the amount of loan which has to be paid.

3.3.1. Impact of solar multiple (SM)

A higher SM increases solar field area thus resulting in higher field thermal output. With increasing SM, a sharp increase in AEP can be observed. This trend continues until field thermal output is sufficient to operate power plants at their rated capacities. The excessive field thermal output is then stored in TES to be used later when needed. After that, the hike in AEP is relatively less intense.

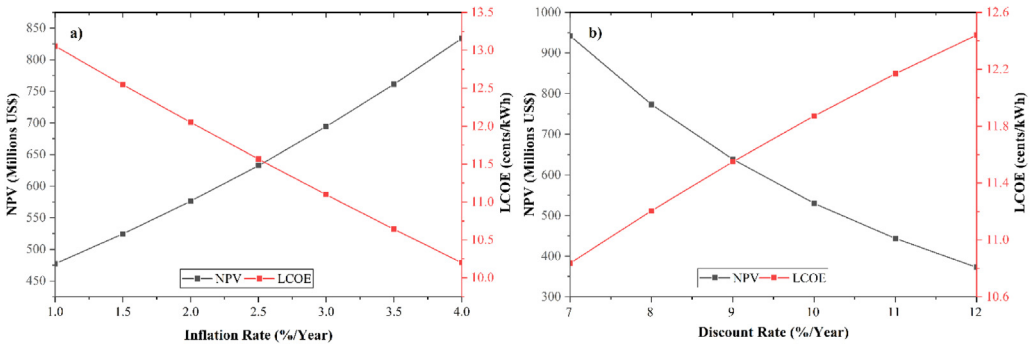

Fig. 12. Sensitivity analysis carried out on (a) inflation rate and (b) discount rate for CSP system.

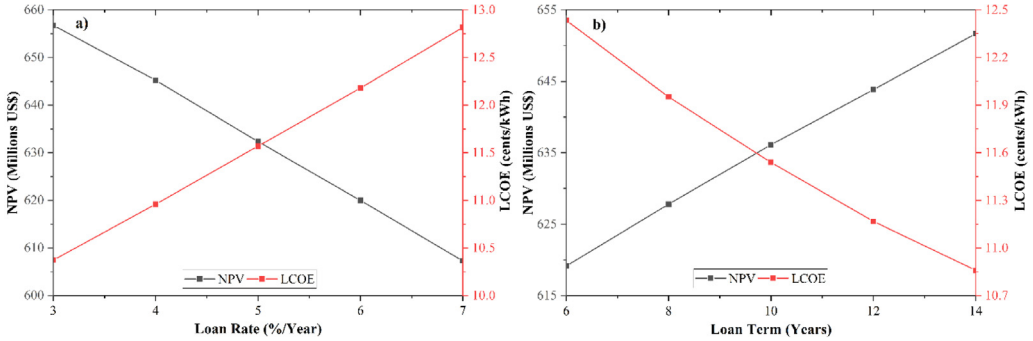

Fig. 13. Sensitivity analysis carried out on (a) loan rate and (b) loan term for CSP system.

To find the impact of SM on the techno-economic viability of the project, the value of SM varied from 1.0 to 4.0 with an interval of 0.25. The Fig. 14 shows the variation in annual energy production based on SM and hours of TES. For a specified TES, the value of AEP increases rapidly with increasing SM at an initial stage. This trend continues until field thermal output is sufficient to run the plant with or without TES at its design capacity. After that, the increase in AEP becomes less intense with a further increase in SM. Thus, initially increasing SM contributes to larger field thermal power output which results in a sharp increase in the value of AEP at the initial stage but a further increase in SM attributes more to field thermal losses than AEP.

3.3.2. Impact of Thermal Energy Storage (TES)

Having a larger TES is not always beneficial for each solar field size. Thus, it is essential to determine the optimal TES capacity for each SM concerning the viability of CSP plants from an economic perspective. The capacity of thermal energy storage (TES) varies from 0 to 15 h with an interval of 1 h. To assess the impact of TES capacity on techno-economic viability, the variation of AEP is shown in Fig. 15. Based on the following figure, an increase in the capacity of TES has no significant impact on AEP for the plants with SM of 1.0 because field aperture area can only provide sufficient field thermal output to run power block at its rated capacity under the design conditions. Therefore, there is no excessive field thermal output for storing in TES to generate electricity during no sunshine hours. Consequently, an increase in TES shows no impact on AEP for power plants with SM of unity.

When SM starts increasing from 1.0, the impact of TES can be seen on the values of AEP and LCOE. For such cases, the excessive field thermal output is used to charge TES for producing power during cloudy or nighttime. Accordingly, the amount of AEP increases, and consequently, the value of LCOE decreases. This trend continues until all the excessive field thermal output is stored in a storage system. After that, a further increase in TES capacity shows no significant impact on AEP, and it only increases the storage cost, and as a result, the value of LCOE starts increasing as discussed earlier in Fig. 11. Thus, an optimal TES size can be determined against each SM according to the objective of minimized LCOE. The optimal TES size increases with an increase in SM, so the power plants with higher SM should have larger TES capacity for the sake of economic viability. Table 9 shows the optimized TES capacity against each SM value. This optimal TES size against each step of SM is based on the objective function of minimized LCOE.

3.3.3. Impact of cooling system

CSP plants require water for mirror washing, as well as for cooling purposes. About 6% of the total water is used for mirror washing purposes in this work, while the rest is consumed by cooling CSP plants. In this study, two types of cooling systems, air-cooled and water-cooled condensers have been investigated. Since the air-cooled condenser works on dry bulb temperature and the water-cooled works on wet bulb temperature. The performance of a CSP plant improves by replacing an air-cooled condenser with an evaporative condenser, but water usage increases exponentially. The wet cooling system increases the AEP by almost 5% and decreases the LCOE by 4.5%. However, wet cooling systems consume water much more than dry cooling systems. Table 10 indicates that water usage for a power plant with a dry cooling system is 94% less than that for a plant with a wet cooling system. The average water requirement for dry cooling is 0.3 m^3/MWh, while it exceeds up to 3.7 m^3/MWh in case of wet cooling, which is in accordance with published studies (Moris et al., 2021). So, CSP plants with evaporative condensers have slightly better efficiency and can be built in regions where water is excessively available. But there is no justification for using wet cooling systems for the regions which suffer from the water shortage. It is to be noted that water costs are not considered in the evaluation of condenser type.

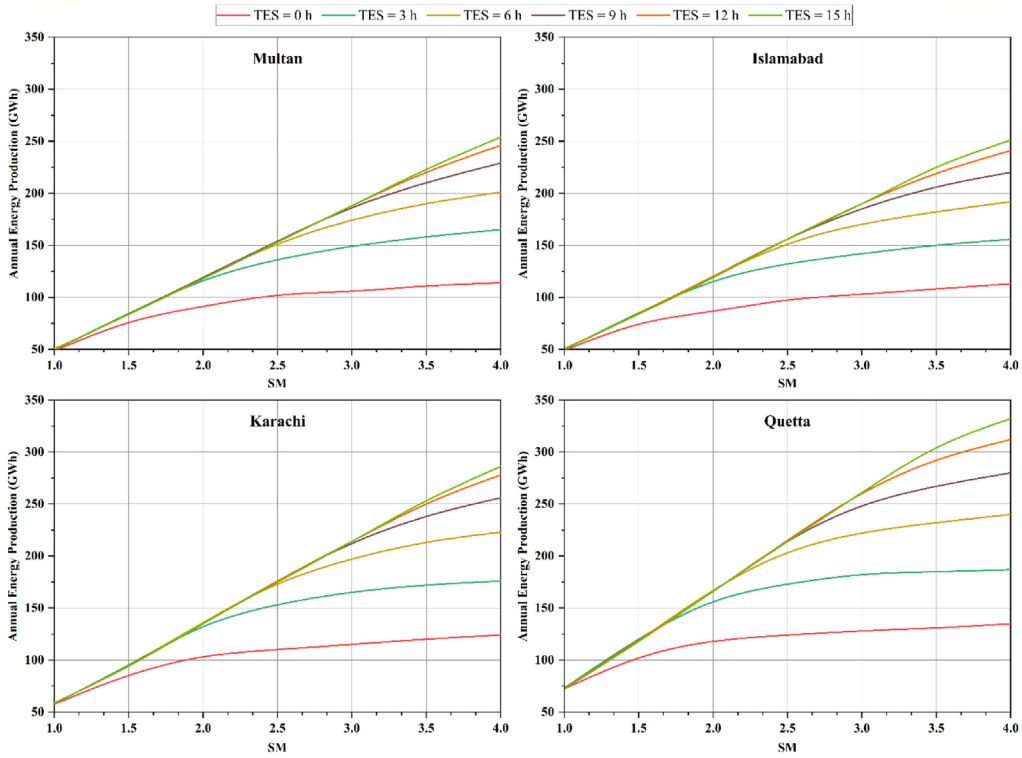

Fig. 14. The impact of SM on AEP of four selected sites for CSP.

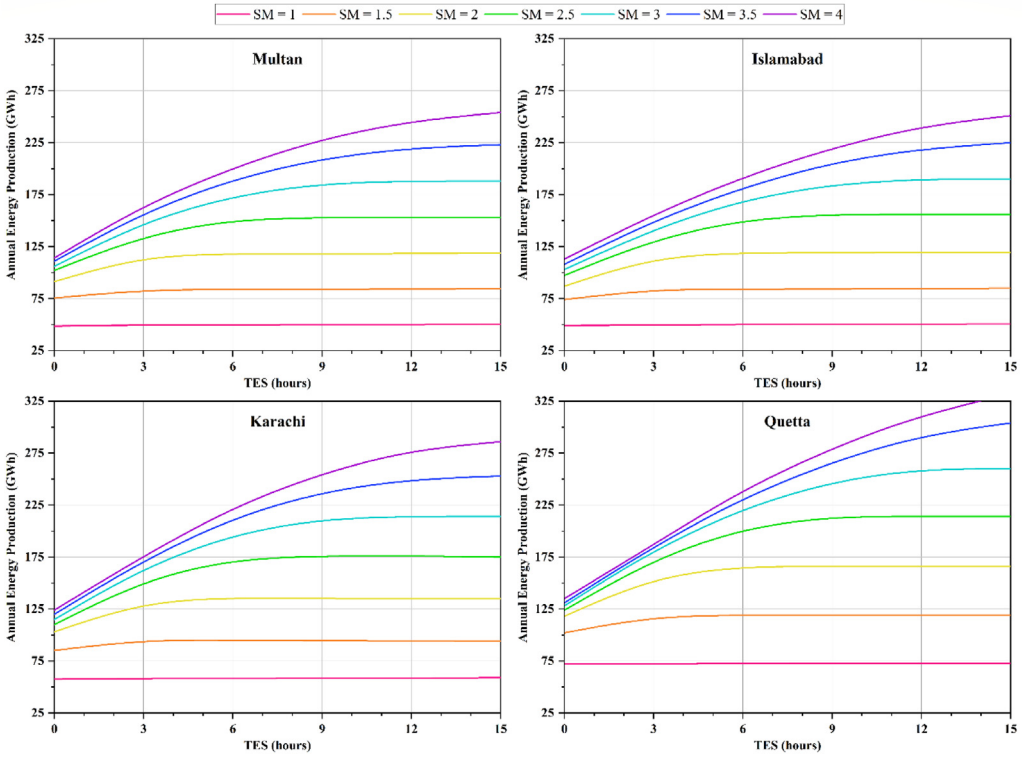

Fig. 15. The impact of TES on AEP of four selected sites for CSP.

3.4. Performance evaluation of the PV system

In this section, performance evaluation of Photovoltaic (PV) is presented and discussed. The monthly average ambient temperature and wind speed are shown in Fig. 7. The daily average ambient temperature is 18.7 °C, with average minimum and maximum temperatures varying from −2 °C in January to 35 °C in July. The monthly average ambient temperature changes from 4.7 °C in January to 29.5 °C in July. The daily sunshine hours vary from 7 to 11 for winter and summer, respectively. The Fig. 16

Table 9
Values of AEP, CF, LCOE, PBP, and water usage with optimal TES based on the minimum LCOE.

Location	SM	Optimal TES (h)	LCOE (¢/kWh)	AEP (GWh)	CF (%)	PBP (Years)	Water used $\times 10^3$ (m^3)
Multan	1.0	0	23.6	48.5	11.1	12.36	20.0
	1.5	1	18.5	83.1	19.2	10.4	30.5
	2.0	3	17.2	116.0	26.5	9.9	40.7
	2.5	5	16.6	148.7	33.8	9.6	50.6
	3.0	8	16.3	183.8	41.9	9.5	61.2
	3.5	10	16.1	214.4	49.1	9.4	71.1
	4.0	12	15.9	246.6	56.2	9.3	81.2
Islamabad	1.0	0	22.7	49.1	11.2	12.0	19.1
	1.5	1	18.1	83.4	19.0	10.3	29.2
	2.0	3	17.0	115.4	26.3	9.8	39.2
	2.5	5	16.3	146.9	33.7	9.5	48.4
	3.0	8	16.0	181.6	41.5	9.4	58.3
	3.5	10	15.9	211.4	48.2	9.3	68.1
	4.0	12	15.7	241.7	55.1	9.2	77.3
Karachi	1.0	0	19.1	57.5	13.1	10.8	19.6
	1.5	1	15.5	94.2	21.5	9.2	29.4
	2.0	3	14.4	132.3	30.3	8.7	39.6
	2.5	5	13.8	169.5	38.6	8.5	49.6
	3.0	8	13.6	209.6	47.8	8.4	59.6
	3.5	10	13.4	244.8	55.8	8.3	69.5
	4.0	13	13.3	282.1	64.6	8.3	79.5
Quetta	1.0	0	14.0	72.4	16.5	8.6	18.7
	1.5	1	11.7	115.8	26.3	7.5	28.3
	2.0	4	11.0	163.2	37.2	7.2	38.1
	2.5	7	10.8	209.3	47.8	7.1	48.0
	3.0	10	10.7	254.7	58.0	7.1	57.2
	3.5	12	10.6	292.5	66.8	7.0	66.5
	4.0	14	10.6	330.4	75.4	7.0	75.3

Table 10
Impact of condenser type on the performance of solar thermal power generation.

Location	Condenser type	Annual energy (GWh)	Capacity factor (%)	LCOE (¢/kWh)	Water usage (m^3/MWh)
Multan	Air-cooled	112.77	25.7	18.46	0.36
	Evaporative	119.06	27.2	17.53	4.02
Islamabad	Air-cooled	113.35	25.9	17.82	0.34
	Evaporative	119.26	27.3	16.96	3.86
Karachi	Air-cooled	129.21	29.5	15.47	0.31
	Evaporative	135.33	30.9	14.78	3.67
Quetta	Air-cooled	160.27	36.6	11.57	0.27
	Evaporative	168.01	38.4	11.05	3.42

Table 11
PV system performance variation by tracking mode.

Tracking mode	Fixed tilt	One axis	Two axis
Energy (GWh)	86.51	100.89	112.92
Capacity factor (%)	19.8	23	25.8
Energy yield (kWh/kW)	1730	2018	2259

shows the month-wise performance of a solar photovoltaic power plant of the same capacity. The highest monthly energy of 7.71 GWh is produced in May with a capacity factor of 20.72% while the lowest 5.68 GWh is produced in February with a 16.34% plant capacity factor. PV system specific yield recorded as 1,730 kWh/kW.

A tracking system improves energy yield of PV system, but it costs additional capital cost to deploy trackers. The parametric simulation showed that 31° is the optimum tilt angle for a solar PV system in Quetta. Table 11 shows the difference in energy yield with fixed, one axis, and two axis tracking systems. By keeping the economic feasibility in view, the single-axis tracking system performs better as two-axis tracking system costs about 70% more (Sajid et al., 2022).

Studies show that thin-film modules perform better from performance perspective while crystalline silicon modules perform better from economic perspective. Thus, Thin film modules perform extraordinary at high ambient temperature because of the lower temperature coefficient of modules which makes them a suitable choice for tropical climate regions.

3.5. Economic evaluation of the PV system

In order to determine the feasibility of any energy project, it is very crucial to perform the economic evaluation of that project. System cost and other economic parameters of PV plant are presented in Tables 7 and 8, respectively. Results indicate that the installed PV plant in Quetta performs better from an economic perspective. This is due to the reason that PV systems have much lower upfront capital cost as compared to CSP technology. The sizeable negative cash flow at the initial stage of the project indicates the investment cost of the project. The positive cash flow in the next stage indicates the revenue generated through the PV plant by selling electricity to the grid. The levelized tariff of the PV plant is 4.69 cents/kWh with a payback period of 4.1 years. The NPV value of 475.32 million US$ shows that this project is economically feasible.

3.6. Sensitivity analysis of the PV system

The sensitivity analysis of PV is also carried out on inflation rate and discount rate and a similar trend to CSP is observed. The inflation rate from 1.0 to 4.0% and the discount rate from 7.0 to 12.0% are varied to find the economic viability of the project. The

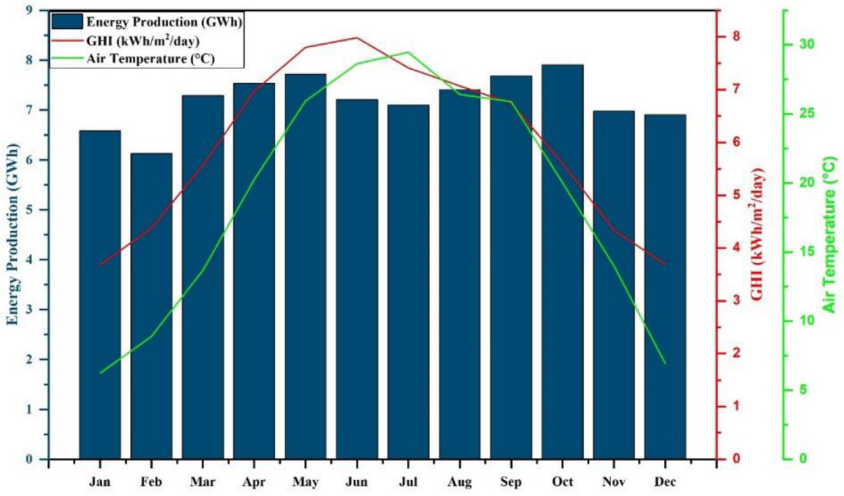

Fig. 16. Monthly energy generation and capacity factor of the solar PV plant in Quetta.

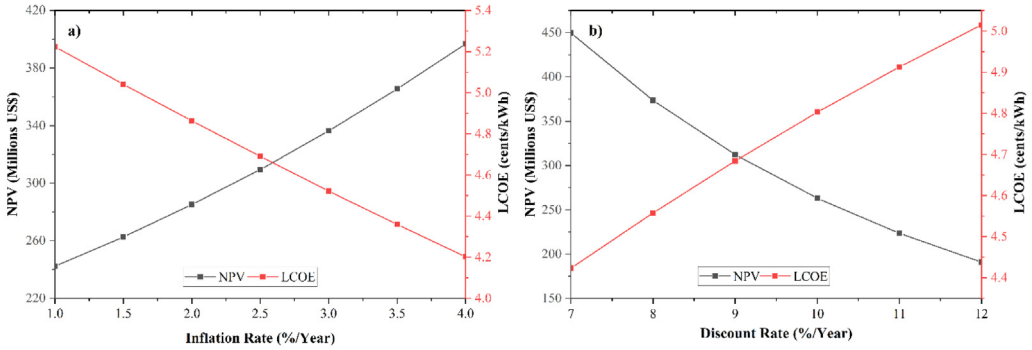

Fig. 17. Sensitivity analysis carried out on (a) inflation rate and (b) discount rate for PV system.

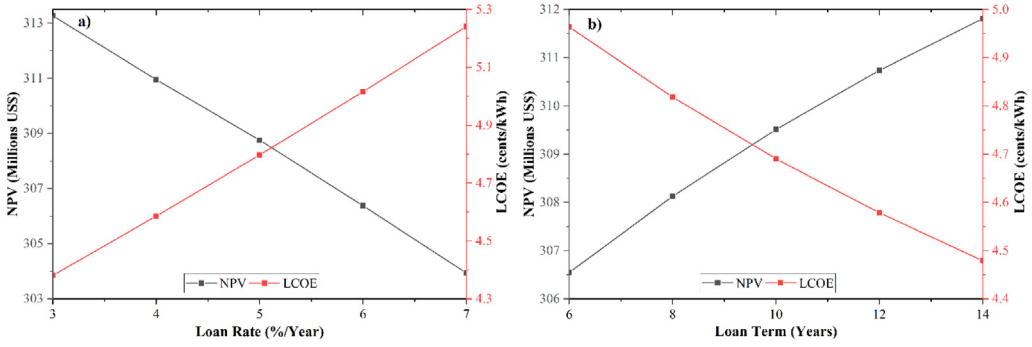

Fig. 18. Sensitivity analysis carried out on (a) loan rate and (b) loan term for PV system.

increase in the inflation rate from 1.0 to 4.0% results in decrease in LCOE and increase in NPV. By varying discount rate from 7.0 to 12.0% results in a change in LCOE from 4.43 ¢/kWh to 5.02 ¢/kWh and NPV from 449 to 190 million US$ as shown in Fig. 17. The sensitivity analysis performed on loan rate indicates that LCOE increases with increase in loan rate, while it decreases with loan term as shown in Fig. 18.

3.7. Environmental analysis

This section identifies the environmental impacts of CSP and PV plants to generate electricity in selected sites. The power sector is considered one of the main reasons for GHG emissions in most parts of the world because of its huge dependence on fossil fuel based thermal power generation. The global energy mix is dominated by fossil fuels which account for more than 80% of energy consumption. GHG emissions can possibly be reduced by deploying cleaner energy technology such as alternative and renewable (ARE). In order to formulate an energy policy with an aim to mitigate GHG emissions and devise an environmental strategy to deter climate change impact, it is provident to accurately estimate GHG emissions from fossil fuel-based plants.

Thus, a weighted average baseline scenario is determined to forecast GHGs emissions from the power sector and mitigate those emissions. This baseline emission factor is determined by analyzing the data of power generation plants, their efficiencies, and fuel consumption proportion (Yousuf et al., 2014). In this study, a base case of weighted average GHG emission electricity

Table 12
Annual GHG emission reduction figures.

Solar technology	PV	CSP			
Location	Quetta	Quetta	Karachi	Islamabad	Multan
Annual energy (GWh)	86.51	160.31	129.26	113.42	112.04
Capacity factor (%)	19.8	36.6	29.5	25.9	25.6
GHG emissions reduced (tCO_2)	45,606	81,423	65,627	57,619	56,951
Crude oil saved (Barrels)	106,059	189,355	152,622	133,997	132,445

system is compared with a proposed case of solar photovoltaic and thermal power plants. The baseline weighted average GHG emission factor of the current energy mix scenario stands at 518 gCO_2/kWh for Pakistan, while the GHG emission factor of the life cycle of solar power stands at 16–40 gCO_2/kWh in most cases (Lamnatou and Chemisana, 2017; Turney and Fthenakis, 2011). GHG emission analysis shown in Table 12 is performed on RETScreen. These are calculated as tons of CO_2 avoided or barrels of crude oils not consumed annually because of the use of renewable energy technology instead of fossil fuel based thermal plants. The GHG emissions and fossils fuel saved (FFS) are approximated from Eqs. (9) and (10), respectively. Where A_{rate} is activity rate, F_e is emission factor, η_{er} is emission reduction efficiency, EG is electricity generated, η_{th} is thermal efficiency, and NCV is net calorific value of fossil fuel.

$$E_{GHG} = A_{rate} \times F_e \times \left(\frac{1-\eta_{er}}{100}\right) \tag{9}$$

$$FFS = \frac{EG}{\eta_{th} \times NCV} \tag{10}$$

Results indicate that a 50 MW CSP based solar thermal plant in Quetta will reduce 81,423 tCO_2 annual emissions that are equivalent to 189,355 barrels of crude oil consumed. Therefore, these renewable energy projects are a viable source of energy security because country had to import a huge chunk of petroleum products. The complete life cycle water consumption (WC) coefficient for dry-cooled and wet-cooled PT solar thermal plants is 0.9 and 3.98 m^3/MWh, respectively; while it stands at 0.33 for PV crystalline silicon (Ali and Kumar, 2017).

3.8. Comparison of CSP and PV

Quetta is the most feasible site for both solar technologies in terms of NPV. Plant simulation for one year shows that the same capacity of CSP and PV plants for Quetta produce 160.31 GWh and 86.59 GWh energy, respectively. The capacity factor for solar PV is 19% while it reaches up to 36.6% in the case of the CSP plant. In terms of economic performance, LCOE of CSP power plant is relatively higher due to its almost 5 times higher capital cost. The land area required to build a CSP plant is larger as compared to PV plant of an equivalent capacity. The simple payback period of the most feasible site for CSP plant is 7.7 years as compared to 4.1 years for PV plant.

As CSP systems can produce power during periods of little to no sunlight hours, their penetration in the energy market can be increased to overcome intermittent problems. Meanwhile, PV systems are not capable of storing thermal energy since they directly convert sunlight into electricity. So, in terms of energy storage and efficiency, CSP technology is better. On the other hand, PV systems are favored due to their much lower capital cost and being easier to build. A comparison of CSP and PV plants from performance and economic perspectives is shown in Table 13.

4. Model validation

Table 14 compares the performance of CSP and PV plants at Quetta, the most practical location, with previous research. Results are verified for both PV and CSP facilities in terms of CF and LCOE. The average variation in CF and LCOE from literature work for the CSP model is 7.4% and 2.8%, respectively. Corresponding to this, the PV model exhibits average deviations in LCOE and CF of 6.9% and 0.79 percent, respectively. This demonstrates that simulated model is capable of reasonably accurate analysis of CSP and PV performance.

Table 13
Comparison of CSP and PV plant from performance and economic perspective.

	CSP	PV
Annual energy (GWh)	160.31	86.51
Capacity factor (%)	36.6	19.8
LCOE (cents/kWh)	11.57	4.69
Payback period (Years)	7.7	4.1
Generation (Acres/GWh/year)	2.77	2.33
Capacity (Acres/MW)	8.8	4.06
Solar to electrical efficiency (%)	14.2	20.8
GHG emissions reduction (tCO_2)	93,924	50,812
Net present value (USD)	632,201,256	309,303,456

5. Conclusion

The prospects of deploying solar power technology in terms of technical, economic, and environmental perspectives are analyzed for four selected locations of different climate zones in Pakistan. The availability of high solar irradiance, land, water, infrastructure, and grid connectivity makes a location feasible for solar thermal power plants, while ambient temperature and wind speed play a critical role in the performance of solar PV plant. A study of 50 MW CSP and PV based power plants is simulated for a lifetime period of 25 years. Solar thermal power generation is found to be technically and economically viable for locations with an average daily DNI greater than 5 kWh/m^2 and a slope angle of no more than 3%. Simulation results show that the northwestern part of Baluchistan is very promising for CSP deployment due to the availability of high solar irradiance. Out of selected sites, Quetta performed better in terms of both technical and financial aspects due to its high solar irradiance availability for CSP and low average ambient temperature for PV based power plant. For Quetta, the annual energy production of CSP is 160.27 GWh with capacity factor of 36.6% while it is 86.59 GWh with capacity factor of 19% for solar PV. The LCOE for CSP power plant is 11.57 cents/kWh with a payback period of 7.7 years while it is 4.69 cents/kWh with a payback period of 4.1 years for solar PV. CSP plant has superior annual energy production and capacity factor in comparison to PV plant, while PV plant is superior in terms of project capital cost and levelized cost of energy. Thus, it indicates that CSP technology performs better from technical perspective, while PV technology performs better from economic perspective. Lack of awareness about the adverse impacts of fossil fuel-based power plants on the environment and no interest in shifting towards renewable energy sources is a primary hurdle in adopting clean and green energy. Furthermore, infrastructure upgradation is needed to improve the flexibility of national grid to accommodate the substantial proportions of renewable energy.

Overall, this research work can be used as a reference to carry out the techno-economic and environmental assessment of

Table 14
Performance comparison of CSP and PV plant with literature work.

Author	Location	Capacity	Type	CF (%)	LCOE (¢/kWh)	Reference
This work	**Quetta, Pak**	**50 MW**	**CSP**	**36.5**	**11.6**	
Tahir et al.	Quetta, Pak	100 MW	CSP	31.7	14.7	Tahir et al. (2021)
Hirbodi et al.	Shiraz, Iran	50 MW	CSP	45.1	15.4	Hirbodi et al. (2020)
Awan et al.	Tabuk, KSA	100 MW	CSP	45.4	10	Awan et al. (2019)
This work	**Quetta, Pak**	**50 MW**	**PV**	**19.8**	**4.69**	
Awan et al.	Tabuk, KSA	100 MW	PV	30.2	3.6	Awan et al. (2019)
Mukisa et al.	Kampala, UG	25.4 MW	PV	14.3	5.75	Mukisa et al. (2019)
Ali & Khan	Lahore, Pak	42 kW	PV	14.8	4.93	Ali and Khan (2020)

other CSP technologies such as solar power tower, parabolic dish, and linear fresnel reflectors. This analysis provides baseline for comparative analysis of two different solar technologies' potential at any given location.

CRediT authorship contribution statement

Asad Ullah: Conceptualization, Methodology, Investigation, Formal analysis, Supervision, Validation, Writing – original draft, Writing – review & editing. **Mariam Mahmood:** Conceptualization, Methodology, Investigation, Formal analysis, Supervision, Validation, Writing – original draft, Writing – review & editing. **Sheeraz Iqbal:** Conceptualization, Methodology, Investigation, Formal analysis, Supervision, Validation, Writing – original draft, Writing – review & editing. **Muhammad Bilal Sajid:** Conceptualization, Methodology, Investigation, Formal analysis, Supervision, Validation, Writing – original draft, Writing – review & editing. **Zohaib Hassan:** Conceptualization, Methodology, Investigation, Formal analysis, Supervision, Validation, Writing – original draft, Writing – review & editing. **Kareem M. AboRas:** Conceptualization, Methodology, Investigation, Supervision, Formal analysis, Validation, Writing – original draft, Writing – review & editing. **Hossam Kotb:** Conceptualization, Methodology, Investigation, Formal analysis, Supervision, Validation, Writing – original draft, Writing – review & editing. **Mokhtar Shouran:** Methodology, Visualization, Resources, Funding acquisition, Writing – review & editing. **Bdereddin Abdul Samad:** Methodology, Visualization, Resources, Funding acquisition, Writing – review & editing.

Declaration of competing interest

The authors declare that they have no known competing financial interests or personal relationships that could have appeared to influence the work reported in this paper.

Data availability

No data was used for the research described in the article.

References

Agyekum, E.B., 2021. Techno-economic comparative analysis of solar photovoltaic power systems with and without storage systems in three different climatic regions, Ghana. Sustain. Energy Technol. Assess. 43 (November 2020), 100906. http://dx.doi.org/10.1016/j.seta.2020.100906.

Ahmed, N., et al., 2021. Techno-economic potential assessment of mega scale grid-connected PV power plant in five climate zones of Pakistan. Energy Convers. Manage. 237, 114097. http://dx.doi.org/10.1016/j.enconman.2021.114097.

Akhter, M.N., Mekhilef, S., Mokhlis, H., Olatomiwa, L., Muhammad, M.A., 2020. Performance assessment of three grid-connected photovoltaic systems with combined capacity of 6.575 kWp in Malaysia. J. Clean. Prod. 277, 123242. http://dx.doi.org/10.1016/j.jclepro.2020.123242.

Aksoy, L., 2009. The impact of electric vehicles on electricity consumption. Accessed: May 13, 2022. [Online]. Available: https://energypost.eu/the-impact-of-electric-vehicles-on-electricity-demand/.

Ali, H., Khan, H.A., 2020. Techno-economic evaluation of two 42 kWp polycrystalline-Si and CIS thin-film based PV rooftop systems in Pakistan. Renew. Energy 152, 347–357. http://dx.doi.org/10.1016/j.renene.2019.12.144.

Ali, B., Kumar, A., 2017. Development of water demand coefficients for power generation from renewable energy technologies. Energy Convers. Manage. 143, 470–481. http://dx.doi.org/10.1016/j.enconman.2017.04.028.

Alshare, A., Tashtoush, B., Altarazi, S., El-Khalil, H., 2020. Energy and economic analysis of a 5 MW photovoltaic system in northern Jordan. Case Stud. Therm. Eng. 21 (November 2019), 100722. http://dx.doi.org/10.1016/j.csite.2020.100722.

Awan, A.B., Zubair, M., Praveen, R.P., Bhatti, A.R., 2019. Design and comparative analysis of photovoltaic and parabolic trough based CSP plants. Sol. Energy 183 (March), 551–565. http://dx.doi.org/10.1016/j.solener.2019.03.037.

Belgasim, B., Aldali, Y., Abdunnabi, M.J.R., Hashem, G., Hossin, K., 2018. The potential of concentrating solar power (CSP) for electricity generation in Libya. Renew. Sustain. Energy Rev. 90 (March), 1–15. http://dx.doi.org/10.1016/j.rser.2018.03.045.

Bishoyi, D., Sudhakar, K., 2017. Modeling and performance simulation of 100 MW PTC based solar thermal power plant in Udaipur India. Case Stud. Therm. Eng. 10 (2017), 216–226. http://dx.doi.org/10.1016/j.csite.2017.05.005.

Boukelia, T.E., Mecibah, M.S., Kumar, B.N., Reddy, K.S., 2015. Optimization, selection and feasibility study of solar parabolic trough power plants for Algerian conditions. Energy Convers. Manage. 101, 450–459. http://dx.doi.org/10.1016/j.enconman.2015.05.067.

Cozzi, L., Gould, T., 2021. World Energy Outlook 2021. IEA Publ., pp. 1–386, [Online]. Available, www.iea.org/weo.

Crespi, F., Sánchez, D., Rodríguez, J.M., Gavagnin, G., 2020. A thermo-economic methodology to select sCO2 power cycles for CSP applications. Renew. Energy 147, 2905–2912. http://dx.doi.org/10.1016/j.renene.2018.08.023.

D. of E. and S. Affairs, 2019. World population prospects 2019. no. 141.

Dersch, J., et al., 2004. Trough integration into power plants-a study on the performance and economy of integrated solar combined cycle systems. Energy 29 (5–6), 947–959. http://dx.doi.org/10.1016/S0360-5442(03)00199-3.

Elmohlawy, A.E., Ochkov, V.F., Kazandzhan, B.I., 2019. Thermal performance analysis of a concentrated solar power system (CSP) integrated with natural gas combined cycle (NGCC) power plant. Case Stud. Therm. Eng. 14 (May), 100458. http://dx.doi.org/10.1016/j.csite.2019.100458.

GoP, 2006. Policy for development of renewable energy for power generation: Employing small hydro, wind, and solar technologies. Minist. Water Power Gov. Pak. 44.

Hall, F., Greeno, R., 2019. Alternative and renewable energy. Build. Serv. Handb. 641–660. http://dx.doi.org/10.4324/9780080969831-16.

Henner, D., REN21, 2017. Ren21.

Hirbodi, K., Enjavi-Arsanjani, M., Yaghoubi, M., 2020. Techno-economic assessment and environmental impact of concentrating solar power plants in Iran. Renew. Sustain. Energy Rev. 120 (March 2019), 109642. http://dx.doi.org/10.1016/j.rser.2019.109642.

2021. World Energy Transitions Outlook: 1.5 °C Pathway. [IRENA] - International Renewable Energy Agency.

Kannan, N., Vakeesan, D., 2016. Solar energy for future world: - A review. Renew. Sustain. Energy Rev. 62, 1092–1105. http://dx.doi.org/10.1016/j.rser.2016.05.022.

Kassem, A., Al-Haddad, K., Komljenovic, D., 2017. Concentrated solar thermal power in Saudi Arabia: Definition and simulation of alternative scenarios. Renew. Sustain. Energy Rev. 80 (2016), 75–91. http://dx.doi.org/10.1016/j.rser.2017.05.157.

Khalid, A., Junaidi, H., 2013. Study of economic viability of photovoltaic electric power for Quetta e Pakistan. Renew. Energy 50, 253–258. http://dx.doi.org/10.1016/j.renene.2012.06.040.

Lamnatou, C., Chemisana, D., 2017. Concentrating solar systems: Life Cycle Assessment (LCA) and environmental issues. Renew. Sustain. Energy Rev. 78 (May), 916–932. http://dx.doi.org/10.1016/j.rser.2017.04.065.

Moris, C.H., Guevara, M.T.C., Salmon, A., Lorca, A., 2021. Comparison between concentrated solar power and gas-based generation in terms of economic and flexibility-related aspects in chile. Energies 14 (4), http://dx.doi.org/10.3390/en14041063.

Mukisa, N., Zamora, R., Lie, T.T., 2019. Feasibility assessment of grid-tied rooftop solar photovoltaic systems for industrial sector application in Uganda. Sustain. Energy Technol. Assess. 32 (2018), 83–91. http://dx.doi.org/10.1016/j.seta.2019.02.001.

NEPRA, 2020. Determination of National Electric Power Regulatory Authority in the matter of tariff petition filed by Mls. Asia Energy (Private) Ltd. for determination of generation tariff in respect of 30 MWp solar power project (Case no. NEPRAITRF-458IAEPL-2018). p. 28, [Online]. Available: https://nepra.org.pk/tariff/Tariff/IPPs/002SolarIPPs/AsiaEnergy(Private)Ltd/TRF-458AEPLDETERMINATION07-09-202027946-48.PDF.

NEPRA, 2021. National Electric Power Regulatory Authority Islamic Republic of Pakistan NEPRA/RIADG(Tariff)/TRF- 100/XWDISCOs/1080-1082. pp. 3–5, [Online]. Available: https://nepra.org.pk/licensing/Licences/Generation/IPP-2002/EngroPowergenThar/LAG-285Modification-IEngroPowergen14-10-2019.PDF.

NTDC, 2021. Indicative Generation Capacity Expansion Plan (IGCEP) 2021-2030.

T.H.E. State, B. Of, and M.P. Decision, 2014. State Bank of Pakistan, Vol. 1956, no. February, pp. 9–10. Accessed: Oct. 31, 2022. [Online]. Available: https://www.sbp.org.pk/m_policy/index.asp.

Policy, R.E., 2020. Islamabad, the October 02, 2020, vol. 202.

Purohit, I., Purohit, P., 2017. Technical and economic potential of concentrating solar thermal power generation in India. Renew. Sustain. Energy Rev. 78 (2016), 648–667. http://dx.doi.org/10.1016/j.rser.2017.04.059.

Ravi Kumar, K., Krishna Chaitanya, N.V.V., Sendhil Kumar, N., 2021. Solar thermal energy technologies and its applications for process heating and power generation – A review. J. Clean. Prod. 282, http://dx.doi.org/10.1016/j.jclepro.2020.125296.

Rule, T.A., 2013. ESMAP. 2019. Solar Model Adaptation Report - Pakistan. World Bank, Washington, DC, no. May.

Sadati, S.M.S., Qureshi, F.U., Baker, D., 2015. Energetic and economic performance analyses of photovoltaic, parabolic trough collector and wind energy systems for Multan, Pakistan. Renew. Sustain. Energy Rev. 47, 844–855. http://dx.doi.org/10.1016/j.rser.2015.03.084.

Sajid, J., et al., 2022. Energetic, economic, and greenhouse gas emissions assessment of biomass and solar photovoltaic systems for an industrial facility. Energy Rep. 8, 12503–12521. http://dx.doi.org/10.1016/j.egyr.2022.09.041.

Sau, S., et al., 2016. Techno-economic comparison between CSP plants presenting two different heat transfer fluids. Appl. Energy 168, 96–109. http://dx.doi.org/10.1016/j.apenergy.2016.01.066.

Schillings, C., Stokler, S., 2015. Solar Resource Mapping in Pakistan : Solar Modeling Report, no. March.

Shabbir, N., Usman, M., Jawad, M., Zafar, M.H., Iqbal, M.N., Kütt, L., 2020. Economic analysis and impact on national grid by domestic photovoltaic system installations in Pakistan. Renew. Energy 153, 509–521. http://dx.doi.org/10.1016/j.renene.2020.01.114.

Soomro, M.I., Mengal, A., Memon, Y.A., Khan, M.W.A., Shafiq, Q.N., Mirjat, N.H., 2019. Performance and economic analysis of concentrated solar power generation for Pakistan. Processes 7 (9), 575. http://dx.doi.org/10.3390/pr7090575.

Tahir, S., Ahmad, M., Abd-ur Rehman, H.M., Shakir, S., 2021. Techno-economic assessment of concentrated solar thermal power generation and potential barriers in its deployment in Pakistan. J. Clean. Prod. 293, http://dx.doi.org/10.1016/j.jclepro.2021.126125.

Trabelsi, S.E., Chargui, R., Qoaider, L., Liqreina, A., Guizani, A.A., 2016. Techno-economic performance of concentrating solar power plants under the climatic conditions of the southern region of Tunisia. Energy Convers. Manage. 119, 203–214. http://dx.doi.org/10.1016/j.enconman.2016.04.033.

Turney, D., Fthenakis, V., 2011. Environmental impacts from the installation and operation of large-scale solar power plants. Renew. Sustain. Energy Rev. 15 (6), 3261–3270. http://dx.doi.org/10.1016/j.rser.2011.04.023.

Wu, C.F.J., Hamada, M.S., 2011. Experiments: Planning, Analysis, and Optimization, Others, Vol. 552. John Wiley & Sons.

Yousuf, I., Ghumman, A.R., Hashmi, H.N., Kamal, M.A., 2014. Carbon emissions from power sector in Pakistan and opportunities to mitigate those. Renew. Sustain. Energy Rev. 34 (June), 71–77. http://dx.doi.org/10.1016/j.rser.2014.03.003.

Zubair, M., Awan, A.B., Baseer, M.A., Khan, M.N., Abbas, G., 2021. Optimization of parabolic trough based concentrated solar power plant for energy export from Saudi Arabia. Energy Rep. 7, 4540–4554. http://dx.doi.org/10.1016/j.egyr.2021.07.042.